Influence of Propeller Location, Diameter, and Rotation Direction on Aerodynamic Efficiency

J. A. Cole*
Bucknell University, Lewisburg, Pennsylvania 17837
and
T. Krebs,† D. Barcelos,† and G. Bramesfeld‡
Ryerson University, Toronto, Ontario M5B 2K3, Canada

https://doi.org/10.2514/1.C035917

In this Paper, the integrated propeller–wing system design space is investigated to gain insight into the influence of propeller diameter, location, and rotation direction. To conduct this investigation, a methodology is developed that uses the propeller power required during steady-level flight as a metric for efficiency. Full mutual interaction between the propeller and wing are taken into account in the aerodynamic analysis. To ensure that the propeller is not operating off design, it is designed within an iterative trim loop. This approach is then used to investigate the theory that an inboard-up rotating propeller located at the wing tip is the most aerodynamically efficient configuration through the use of a test case. When considering the trimmed propeller power required, the trends for this case indicate that the optimal propeller for this planform is not an inboard-up rotating propeller at the wing tip, but instead is an inboard-down rotating propeller near the root of the wing.

I. Introduction

MANY modern nonconventional aircraft designs prominently feature the interaction between propellers and wings. The X-57 Maxwell [1–3], for example, uses advances in electric motor technology for gains in cruise efficiency through distributed electric propulsion. The NASA GL-10 vertical takeoff and landing unmanned aerial vehicle (UAV) [4] represents a renewed interest in tilt-wing technology. NASA is also investigating the concept of a large civil tiltrotor [5,6] that features a wing that operates nearly entirely in the wake of a large upstream proprotor. A large portion of UAVs are also propeller driven. One particular type of aircraft of interest within this field is the high-altitude long endurance UAV, such as the Defense Advanced Research Projects Agency-sponsored Vulture [7], which features propellers that are distributed across flexible, high-aspect-ratio wings.

Conceptual design of these types of aircraft is particularly challenging because the empirical approaches that are used for conventional aircraft have limited applicability. In addition, the planform and operational design of propellers and wings occur separately in the early phases, using either empirical or simple analytical methods to account for installation effects [8,9]. General trends with respect to the interaction between the two systems were suggested by Prandtl [10], who indicated that placement of the propeller above the wing should increase the wing efficiency, whereas placement of the propeller below the wing should increase propeller efficiency. In-depth physics-based modeling of the interaction between the components, however, is conducted within the preliminary or detailed design phases, when there is limited design freedom to exploit potential aerodynamic benefits. This lack of analysis upstream in the design process adds to the uncertainty with regard to integrated design space.

Several experimental [11–13] and numerical studies [14,15] have indicated significant benefits are available through use of a wing-tip mounted propeller operating inboard up (opposite the tip vortex). As a result and as enabled by advances in electric propulsion, the theory that wing-tip mounted propellers operating inboard up are the most efficient option for a propeller–wing systems has gained traction. One of the stated goals of the AIAA Workshop for Integrated Propeller Prediction (WIPP), for example, is to validate the tip-mounted propeller aerodynamic efficiency benefit [16]. More relevant for this Paper is the example that the X-57 was designed to operate in cruise with wing-tip-mounted propellers only (inboard propellers are designed to fold into the wings during cruise) to increase propulsive efficiency [1,2].

The objective and contribution of this Paper is twofold. First, the authors developed a new approach for conceptual design of propeller–wing systems that takes into account the integrated aerodynamics of the wing and propellers, with a particular focus on ensuring that each propeller–wing system is operating in a trimmed condition and on design. This process allows for a more relevant comparison between competing designs. Second, the authors use this approach to show that the theory that wing-tip mounted propellers operating up inboard are the most efficient configuration is an incomplete picture of the design space and interactional effects. This is accomplished through an investigation of the X-57 in the cruise configuration. A more complete picture of the design space is then provided for this case to gain understanding of the relative sensitivity of the results to the design parameters, and the underlying drivers that result in the optima are explored.

II. Motivation and Background

A review of the studies that support the wing-tip mounting of propellers is helpful to understand both the complexity of the problem and to motivate the authors' methodology. The theory has gained acceptance because there are several studies [11–15] that suggest benefits in various ways. A detailed look into these studies reveals that their conclusions are in fact much more narrow than would be needed to support the general theory.

Snyder and Zumwalt [11] conducted an experiment in which the L/D of a wing-tip-mounted configuration was compared with that of a clean wing (no propeller) to show the advantage of the wing-tip-mounted configuration. In this experiment, the authors describe their approach to determining the wing L/D as follows [11]: "Three component balance data were taken and corrected for direct thrust of the impeller or propeller."

Presented as Paper 2019-2300 at the AIAA Scitech 2019 Forum, San Diego, CA, January 7–11, 2019; received 12 February 2020; revision received 4 June 2020; accepted for publication 11 June 2020; published online Open Access 30 June 2020.

*Assistant Professor, Department of Mechanical Engineering, 1 Dent Drive. Member AIAA.

†Graduate Research Assistant, Department of Aerospace Engineering, 350 Victoria Street. Student Member AIAA.

‡Associate Professor, Department of Aerospace Engineering, 350 Victoria Street. Senior Member AIAA.

This statement indicates that the thrust of the propeller was assumed from a look-up table based on the operating conditions (rotational velocity and V_∞), independent of propeller's location with respect to the wing. The use of a look-up table in this manner neglects the possibly significant impact that a downstream wing can have on the performance of an upstream propeller [15,17]. As a result, it is unclear if the increased L/D is real or a result of a change in thrust due to the propeller location. Snyder and Zumwalt [11] do not discuss a measurement of propeller power required. Thus, in either case, it is unclear what influence the change in L/D had on the power required to achieve that flight condition.

Sinnige et al. [12] performed a considerably more thorough and modern experiment that also quantified the benefit of the wing-tip-mounted propeller over the conventional inboard configuration. In this study, two rectangular wings of similar span (0.748 and 0.730 m) and identical chord (0.240 m) were compared. The first wing featured a midspan (conventional) mounted propeller, and the second wing featured a wing-tip-mounted propeller. The authors found a drag reduction of 15% at set lift and thrust coefficient through use of the tip-mounted configuration. With respect to determining integrated forces, the authors state:

"A simple bookkeeping procedure was followed to separate the forces and moments generated by the wing with nacelle and the propeller. To this end, the isolated propeller's performance data were used, as measured with the sting mounted configuration. In this process, the upstream effect of the wing on the propeller performance was neglected."

Sinnige et al. also assumed propeller power rather than measured it, leading to the previously desribed uncertainties.

Patterson and Bartlett [13] performed experiments on a slightly different (although not unrelated) set of configurations. In this study, three rectangular wings were tested: a baseline clean wing (no propeller, wing area of 2.88 ft^2), the baseline wing with a wing-tip-mounted pusher propeller, and the wing and pusher propeller with an added wing extension. The wing extension effectively results in an inboard-mounted propeller with a wing area of 3.89 ft^2. The authors notably instrumented the propeller shaft to directly measure the propeller thrust independent of the overall model force balance such that the true drag of the model could be calculated. The propeller power required was also directly measured. Unfortunately, power data were omitted from the majority of the results, making it again difficult to parse effects.

A few conclusions from Patterson and Bartlett [13] are noteworthy. First, at a set dimensional thrust, the propeller power required was shown to reduce by approximately 13% from $C_L = 0$ to the $C_L = 0.4$ for the wing-tip-mounted pusher propeller. Adding the wing extension to create an inboard mounted configuration increases the power required at the $C_L = 0$ condition by approximately 10%, which was attributed to increased interference and juncture drag. The power required for this case was relatively insensitive to lift coefficient; thus by $C_L = 0.4$, the difference between the wing-tip-mounted configuration and the inboard configuration was shown to be over 25% in favor of wing-tip mounting. From this, the authors conclude that the pusher propeller located at the wing-tip benefits from the tip vortex interaction (an effect that increases with lift coefficient), whereas the inboard propeller does not. The second noteworthy conclusion was that at a set dimensional thrust, the drag coefficient of the wing itself was reduced significantly from the inboard mounted case to the wing-tip-mounted case (e.g., at $C_L = 0.4$, $\Delta C_D \approx 0.005$), again an approximately 25% reduction.

This study is compelling and certainly has merit, particularly when considered in concert with the previous two. For this wing, a clear benefit can be seen to the tip-mounted pusher propeller configuration. Still, several aspects of the approach are worthy of further discussion including the influence of changing wing area, aspect ratio, and ratio of propeller diameter to wing span between the cases. For example, the wing half-span increased from the baseline wing to the wing with extension by 30%, but the propeller diameter did not change. An argument could be made that this ratio should be held constant, or at least taken into consideration. In addition, if a trim condition were sought, it would require an increase in thrust to offset the increase in dimensional drag due to the increased wing area. Perhaps at this increased thrust, the influence of the wing (and on the wing) would be more significant. Even considering either case alone (not in comparison to one another), if the thrust is held constant but the drag has changed significantly, the change in power required at that value of thrust is irrelevant. If thrust is not equal to drag, the airplane cannot maintain steady-level flight. Similar arguments could be made with respect to lift and weight of an airplane. Finally, the influence of the planform itself was not investigated (i.e., would this benefit be seen on a tapered wing, an elliptical wing, etc.?). Because of these concerns, generalizing the results of the study seems tenuous at best.

The limitations within experimental results are due to both the complexity of the problem itself and the high expenses associated with experimental work. To get a broader view, a few low-order theoretical and numerical methods have been used to investigate the aerodynamic tradeoffs of propeller–wing systems [14,18]. Miranda and Brennan [14] used a purely inviscid, fixed-wake model with assumed span and blade circulation. Three conclusions from this analysis are important to this discussion. First, the inviscid benefits of propeller–wing interaction can be attained with equivalent efficacy through an upstream propeller coupled with a downstream wing, in which case they manifest as a reduction in induced drag, or an upstream wing coupled with a downstream propeller, in which case they manifest as increased thrust. Second, the wing-tip-mounted propeller operating opposite the tip vortex (once again, inboard up) resulted in reduced power requirements for a given flight condition assuming that condition is dictated by thrust being equivalent to drag. Finally, the benefit achieved through use of wing-tip mounting of the propeller is dependent upon the span loading of the wing, with less of a benefit for wings with triangular lift distributions (lightly loaded tips).

A similar inviscid, fixed-circulation model was used by Kroo [18] to investigate design for minimum induced losses in a propeller–wing system. The results of this study were in agreement with Miranda and Brennan [14] in terms of the influence of an upstream versus downstream propeller. Interestingly though, in regard to propeller location, Kroo states, "The propeller's spanwise position plays a small role in wing-propeller interaction, with somewhat greater benefits available as the propeller is moved outboard. [. . .] The vertical location of the propeller disk is of greater importance."

Kroo [18] then proceeds to demonstrate potential benefits of designing the propeller–wing system (both the propeller and wing in combination) for minimum induced losses, resulting in an effective propulsive efficiency of 102% in at least one case. In agreement with the previous studies, this study shows a greater benefit for inboard-up rotation.

Both Kroo [18] and Miranda and Brennan [14] assume fixed circulation distributions, which is to say that mutual interaction between the propeller and wing surfaces is neglected in terms of enforcing flow tangency. They also assume fixed, prescribed wakes, neglecting this component of interaction as well. Finally, neither study accounts for viscous effects. It is interesting that, despite the similarity of their approaches, their conclusions regarding the influence of propeller spanwise location differ from one another.

While aircraft design is undoubtedly a multidisciplinary problem in which the influence of weight, structures, and stability and control cannot be neglected, it is difficult to drive the design process without a general understanding of the aerodynamic trade space of propellers and wings. If, for example, one can achieve a 25% reduction in power required by using a wing-tip-mounted propeller instead of an inboard propeller, perhaps the associated tradeoff in structural weight is worthwhile. Alternatively, if this is only the case for a single planform and propeller design combination and only modest gains are possible for more realistic designs, it is a significantly less attractive option.

There are several important takeaways from this detailed review of the literature on this topic for the stated objectives of this study. First, to usefully compare designs, it is important to ensure that they are operating in steady-level flight conditions. Second, such a comparison must rely on a metric that takes into account the performance of the full system (both the wing and propeller). Third, comparisons must be made using full two-sided interactional effects between the propeller and wing within the aerodynamic analysis to ensure all

influential effects are taken into account. Finally, the theory that the tip-mounted up-inboard rotating propeller is the most efficient configuration is based on studies that are much more narrow in their conclusions and should be viewed with appropriate skepticism.

III. Methodology

The details of the method for design space exploration are provided in this section, starting with a discussion of the metric used to assess aerodynamic efficiency. Next, the complete design process is described in detail. Finally, the aerodynamic method used within the design process is outlined and validated against baseline X-57 data.

A. Metric for Aerodynamic Efficiency

To maximize the aerodynamic efficiency of a propeller–wing system, it is necessary to first identify an appropriate metric for efficiency in steady-level flight. The typical metrics discussed for this purpose with respect to aerodynamic design are the wing lift-to-drag ratio (L/D) and the propeller efficiency. The drawback of using L/D for this application is that it does not take into account any changes in propeller thrust or power resulting from a change in wing design. Likewise, an optimization of propeller efficiency does not account for any resulting changes to lift and drag of the wing. Because the propellers and wing interact with one another, these metrics on their own are not sufficient to determine if a design change has improved the overall system.

One approach to take both the propeller and wing efficiency into account is to consider the propeller power required in steady-level flight [17,19]. Steady-level flight is defined by force equilibrium of the aircraft as a whole (i.e., lift = weight and thrust = drag). In the design space exploration discussed in this Paper, only the propeller–wing system performance is modeled explicitly. Thus, a steady-level flight condition must be identified based only on the propeller and wing performance characteristics.

This can be accomplished through the use of two nondimensional coefficients. The first coefficient is that of excess thrust C_x, defined as

$$C_x = \frac{T\cos(\alpha_t) - D}{(1/2)\rho V_\infty^2 S} \tag{1}$$

where T is the thrust, α_t is the offset of the thrust line from the freestream velocity, D is the wing drag, and S is the wing area. The excess thrust at a given lift condition is physically representative of the allowable drag of the rest of the aircraft such that the trim condition can be met. The second nondimensional coefficient C_L^* is that of the lift coefficient augmented with thrust contributions in the lift direction (again due to the offset of the thrust line from the freestream velocity).

It is worth noting that the use of the trimmed propeller power required is similar to the approach employed by Borer et al. [1], in which a range efficiency multiplier was employed. The range efficiency multiplier is the ratio of the range-specific energy consumption at cruise ($P_{\text{consumed,cruise}}/V_{\text{cruise}}$) of the new design to the baseline design. Using the trimmed propeller power required instead of the range multiplier simplifies the modeling requirements and allows for a clearer assessment of the aerodynamic trade space without the influence of other systems. The current approach does omit the influence of the details of the power storage and distribution system.

B. Design Process

A flow chart of the design and analysis process is provided in Fig. 1. The process begins with the definition of the baseline wing geometry and a selected propeller location and diameter. This information is then used to design the first iteration of the propeller with the thrust required estimated based on the baseline L/D. The detailed design of the propeller is then conducted within QMIL [20], which theoretically results in a minimum-induced-loss propeller geometry.

In the example design space exploration included in this Paper, a sweep of propeller diameters and locations was conducted for a wing and cruise condition based on a recent iteration of the X-57 Maxwell. The range of variables considered in this investigation is provided in Table 1. The assumed values for QMIL are provided in Table 2.

Once the initial geometry is defined, a process to trim the aircraft to achieve a steady-level flight condition is undertaken. This process begins with analyzing the geometry with a higher-order free-wake (HOFW) aerodynamic analysis method to determine lift and drag of the wing and thrust and torque of the propeller. A thorough description of the HOFW method is provided in Sec. III.C. If the predetermined C_x and C_L^* values are met, it indicates that the lift is equivalent to the weight of the baseline vehicle and that the thrust leftover after accounting for the drag of the wing of the current design point is equivalent to that of the rest of the baseline vehicle. In this case, trim has been achieved, and the torque calculated can be converted directly to a propeller power required.

If the trim condition has not been met, an iterative process is undertaken to achieve the trim condition with a propeller operating in as near to an on-design case as possible. To accomplish this, both the angle of attack and propeller design are adjusted toward the trim condition taking into account the offset between the QMIL predicted thrust and that predicted by the HOFW method. The process is then repeated until convergence within 1% of target values is achieved. An example of the convergence process is shown in Fig. 2. In general and for most cases, convergence is achieved within five iterations. It is worth noting that this approach varies from those used previously by the authors [17,19] both because of the inclusion of propeller design within the trim loop and in the more direct trim process.

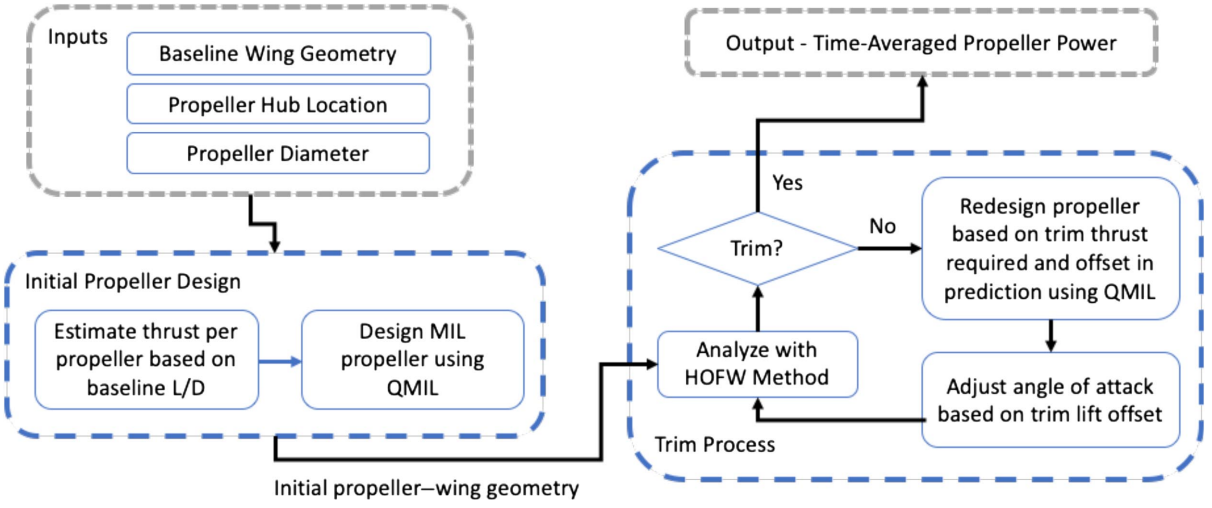

Fig. 1 Flowchart describing analysis for a single case.

Table 1 Variables and ranges for definition of the propeller within the design space exploration

Variable	Range	Constraints/notes
Propeller diameter	0.8 to 1.6 m	0.2 m blade-tip separation, (relevant only near wing root)
Spanwise propeller hub location	Wing root to wing tip	0.2 m blade-tip separation
Vertical propeller hub location	−0.15 to +0.15 m	Below (−) to above (+) leading-edge location
Chordwise propeller hub location	25% of propeller diameter upstream of leading edge	Uniform
Propeller rotation direction	Inboard-up/inboard-down	N/A

Table 2 Assumptions for the propeller design as used with QMIL for the design space exploration

Parameter	Value		Rationale
Hub cutout	18.75%		Baseline
Propeller advance ratio	1.35		Baseline
Design lift coefficients	r/R	c_l	Recommended QMIL values
	0	0.6	
	0.5	0.5	
	1.0	0.4	
Airfoil	MH-117		Baseline airfoil, data constructed from XFOIL

C. Aerodynamic Analysis

1. *Description of Analysis Method*

The aerodynamic analysis method used in this Paper is an incompressible, higher-order, potential flow formulation solved using Neumann boundary conditions. In this case, *higher order* refers to the fact that the elements used to build the potential flow solution consist of greater than zeroth-order distributions of singularity strengths to represent lifting surfaces and their wakes [21]. The method in this Paper uses panels with distributed vorticity, referred to as *distributed vorticity elements* (DVEs) [22,23]. These elements, as depicted in Fig. 3, consist of leading- and trailing-edge vortices that have parabolic spanwise circulation distributions and are connected in the streamwise direction by a vortex sheet with a linearly changing spanwise distribution of vorticity strength.

All lifting surfaces, including fixed surfaces such as wing and tail surfaces, and rotating surfaces such as propeller blades, are represented within the method using nondeforming surface DVEs. Spanwise rows of these elements form lifting lines with bound circulations whose strength changes as second-order splines in the spanwise direction. The Neumann (flow tangency) boundary condition is enforced at control points. Additionally, transitional conditions for circulation and vorticity between neighboring DVEs yield the solution for the strength distribution of the bound circulation.

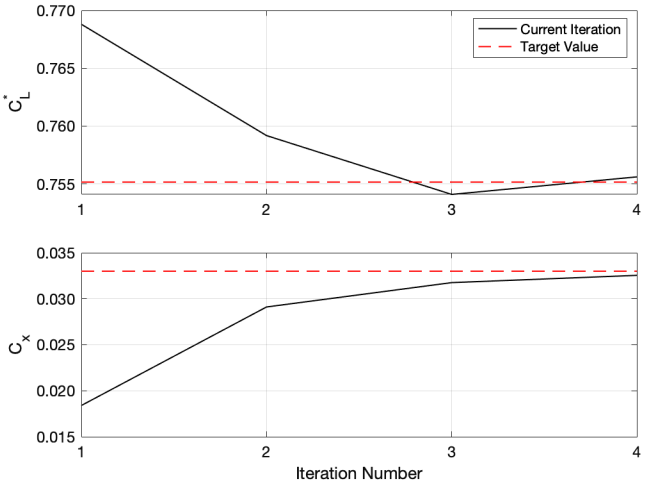

Fig. 2 Example iteration process shown in terms of C_x and C_L^*.

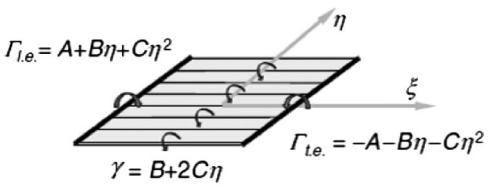

Fig. 3 A visualization of a DVE [22].

The wake of each lifting surface (including propeller blades and fixed-wing surfaces) is developed using a time-stepping approach. During each time step, the lifting surface is advanced a spatial increment, and a row of DVEs is passed into the wake bridging the gap between the wing trailing edge and the wake elements of the previous time steps. The wake is assumed to be quasi-steady, which is to say that trailing vorticity shed from the lifting surface at each time step is propagated throughout the wake. As a result, the leading and trailing-edge filaments on the wake DVEs are omitted from the calculation as they are equal in magnitude and opposite in direction. The subsequent wake representation is a continuous vortex sheet with linearly changing vorticity distribution in the spanwise direction and, as a result, induces finite and realistic velocities everywhere.

The realistic flowfield representation enables the implementation of wake relaxation at each time step to determine the force-free wake geometry. In this process, the wake elements for all surfaces convect and deform based on the local induced velocities. Although the method has relaxed-wake capability, it is not always needed depending on the case. In cases where wake relaxation has a negligible influence the final performance predictions, the use of a fixed-wake assumption significantly reduces computational time.

Once the flowfield solution is determined, the forces on each surface DVE are calculated in the near field using the Kutta–Joukowski theorem. Lift is computed along the lifting lines of the bound circulation considering kinematic velocity of the element and induced velocities. In the case of analysis of a fixed wing, the kinematic velocity is equal and opposite of the freestream velocity. In the case of a rotating surface, such as a propeller blade, the kinematic velocity must also include the rotational velocity. Induced drag is determined along the trailing edge of a lifting surface using the kinematic-velocity component of the cross-product of the circulation shed into the wake at this location and the wake-induced velocities.

Viscous effects in the form of profile drag and nacelle drag are included in the method. Profile drag is taken into account using a table look-up routine. For various sections of the lifting surfaces, tabulated airfoil drag data are interpolated based on the section lift coefficient the local freestream velocity, which is the combination of rotational and freestream speed for propellers. The airfoil data can be based on theoretical predictions or experimental results. The profile-drag modification applies well until major flow separation occurs, for example, near stall and poststall. The nacelle model is that of Shevell [24] and predicts the drag as a function of the ratio of the length to diameter of the nacelle and its wetted area.

This approach to aerodynamic analysis has been used for several applications including formation-flight aerodynamics [25], design of small and micro aerial vehicles [26], design of sailplane winglets [27], and design and analysis of wind turbines [28,29]. For further details on the method as applied to propeller–wing systems including extensive validation, the reader is referred to the work by Cole et al. [17,19].

2. *Baseline Geometry and Validation*

The baseline wing and propeller geometry and operating conditions for this Paper were determined entirely from publicly available

Table 3 Baseline geometry and operating conditions

Parameter	Value
Span	31.6 ft (9.63 m)
Planform area	66.7 ft^2 (6.20 m^2)
Wing loading	45.0 lbf/ft^2 (2154 N/m^2)
Aspect ratio	15.0
Root chord	2.48 ft (0.76 m)
Tip chord	1.74 ft (0.53 m)
Leading-edge sweep	1.9 deg
Cruise propeller diameter	5 ft (1.52 m)
Cruise propeller RPM	2250
Cruise speed	150 kt

data on recent design iterations of the X-57 Maxwell in the cruise configuration. It is worth noting that the multiple inboard propellers on the X-57 are used for high lift takeoff and landing configurations only and are folded into the wings during cruise. Thus, the cruise configuration features only the tip-mounted propellers [1].

The baseline wing geometry is that of Rev3.3 of the aircraft as described by Borer et al. [1]. Key parameters of this geometry are reproduced in Table 3. The propeller geometry is based on an early variant of the cruise propeller geometry provided by Patterson [30] and uses an MH 117 airfoil. The wing airfoil is a modified NASA GA (W)-2, the coordinates for which were found in an OpenVSP model of the aircraft [3]. The drag polars of this airfoil were determined using XFOIL [31] and are provided in Fig. 4.

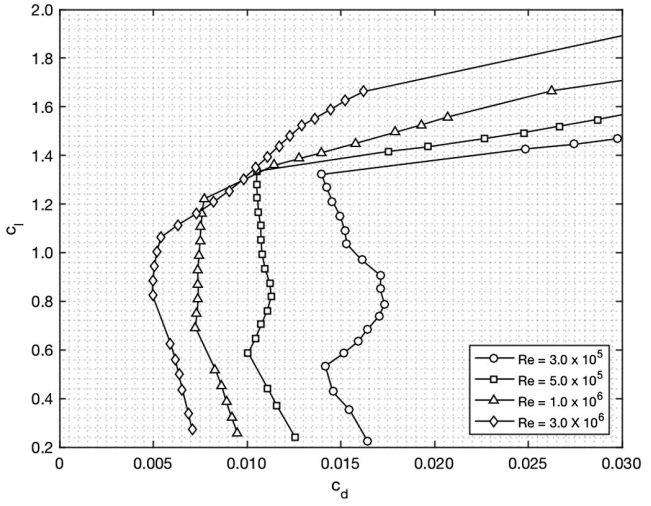

Fig. 4 Drag polars for the wing airfoil as determined using XFOIL.

A visualization of the propeller–wing system as analyzed within the HOFW method is provided in Fig. 5, which shows the lifting surfaces (the wing and propeller blades) in red, the wing wake in blue, and the propeller wake in yellow. To ensure convergence and sufficient resolution, the system was discretized in time and space according to the recommendations of Cole [17] as follows: the wing was modeled with 24 DVEs per half-span (two rows of 12), and the propellers were modeled with a single row of 20 DVEs per blade. The time-step size was set such that a single revolution of the propeller occurs over 20 time steps and all integrated quantities were time averaged over a single revolution of the propeller. For this system, variations in the time-averaged lift, drag, thrust, and torque were less than 0.5% after 140 time steps. To be conservative, the model was run to 160 time steps in all cases.

To validate the performance predictions of this method (referred to as the HOFW method) for this baseline wing and propeller, results were compared with computational fluid dynamics (CFD) results from Borer et al. [2] as shown in Fig. 6. The trim condition for lift and thrust was estimated iteratively through adjusting the angle of attack and propeller blade pitch angle to achieve steady-level flight ($L = W$, $T = D$) over a range of velocities. Because the drag of the full aircraft is needed to trim the thrust but only the wing is modeled within the HOFW method, the drag of the aircraft without the wing was estimated through consideration of L/D estimates provided in Borer et al. [1]. This offset was then added to the drag of the wing as calculated within the HOFW method, and the thrust was trimmed to match the summed quantity.

The results of the HOFW method are within 1% of the Star-CCM+ transitional CFD results in the cruise lift region for both fixed- and relaxed-wake analysis. As the profile drag model in the HOFW approach does account for transition, it is intuitive that the prediction using this approach would be closer to transitional CFD than to fully turbulent CFD. Additionally, the variation between the fixed-wake and relaxed-wake results in this region is minimal. As a result, a fixed-wake assumption was made for the purpose of running the sweep cases as it significantly reduced the computational time per case.

IV. Results and Discussion

The results of the parameter value sweeps described in Table 1 are provided in Figs. 7–9. Each figure depicts a different vertical location of the propeller. The overall minima of the inboard-down and inboard-up configurations are provided as a reference in order to better compare the different plots.

Several points are noteworthy in these plots, starting with Fig. 7. The trends at this vertical location (15 cm below the leading edge) seem to agree with the notion that an inboard-up rotating, wing-tip-mounted propeller is the most efficient option. This result is fairly insensitive to the diameter of the propeller at this location, with a slight advantage in favor of a larger propeller. These results in general agree with the literature.

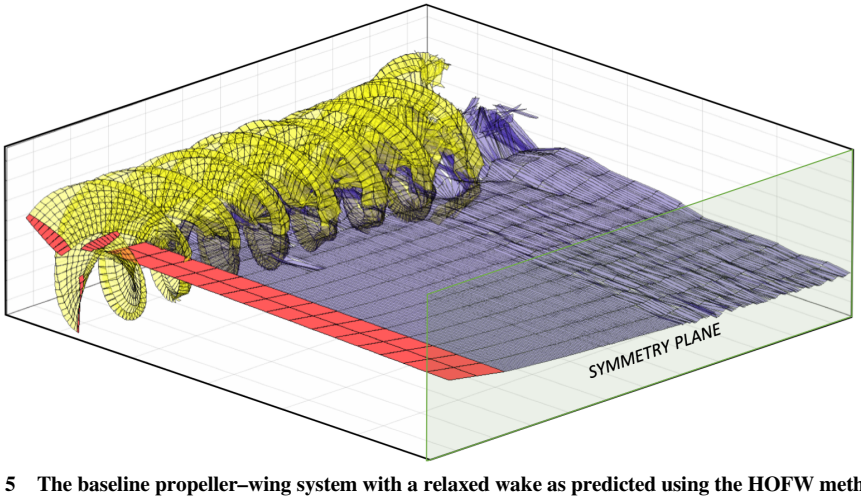

Fig. 5 The baseline propeller–wing system with a relaxed wake as predicted using the HOFW method.

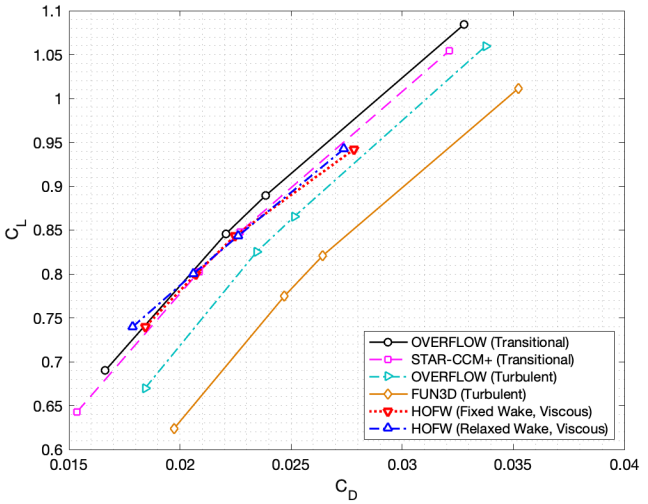

Fig. 6 A comparison of the wing performance as predicted using the HOFW method and as predicted using CFD methods [2].

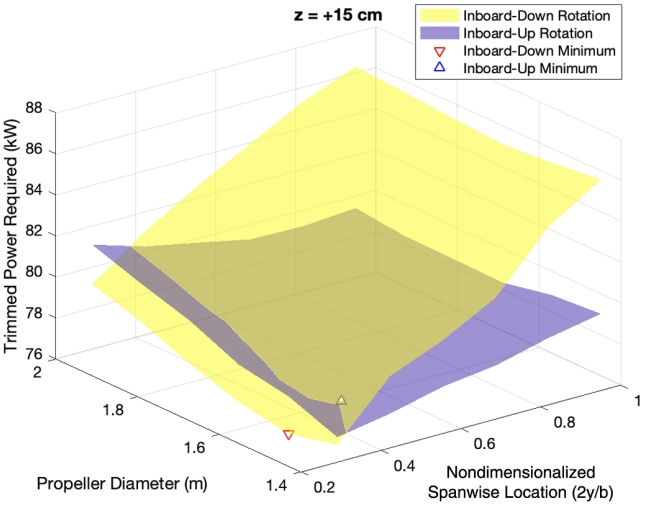

Fig. 9 Time-averaged propeller power as a function of propeller diameter and spanwise location for propeller located 15 cm above leading edge.

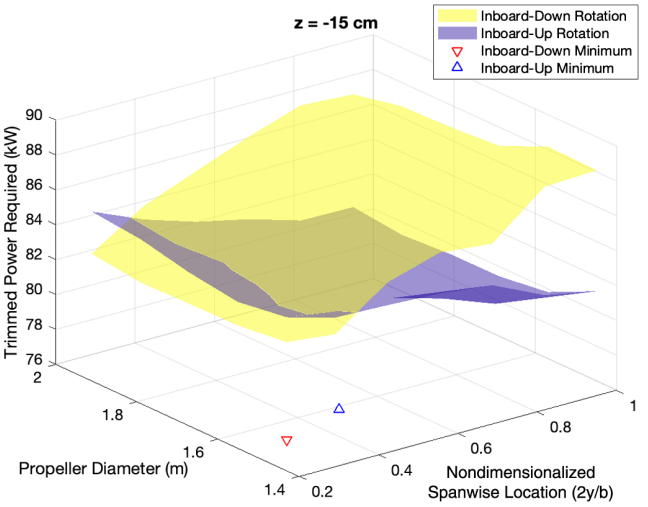

Fig. 7 Time-averaged propeller power as a function of propeller diameter and spanwise location for propeller located 15 cm below leading edge.

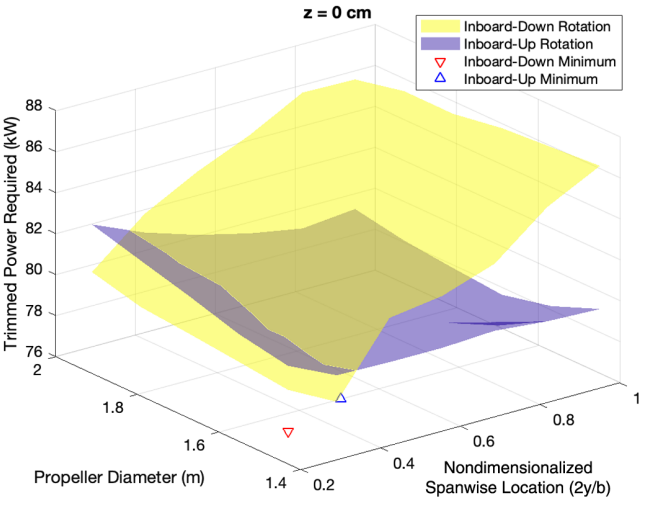

Fig. 8 Time-averaged propeller power as a function of propeller diameter and spanwise location for propeller located in alignment with the leading edge.

The results for the propeller located in the same vertical plane as the leading edge (Fig. 8) are similar in terms of an inboard-up rotating propeller located at the wing tip is the minimum power required case. In comparison with the results provided in Fig. 7 in which the propeller is located below the wing, however, there are two notable changes. First, the average power required in the inboard-up rotation direction is less, which is to say that the configuration is on the whole more efficient at all locations. The benefit of moving the inboard-up rotating propeller towards the wing tip in terms of power required is less than is seen in the below-the-wing case. Because of this, and because there is not an equivalent change in the trends of the inboard-down rotation orientation, the inboard located inboard-down rotating propeller begins to become a competitive design.

Finally, at a location of 15 cm above the leading edge, the inboard-up rotating propeller flattens out entirely, and a clear advantage is shown by the inboard-down rotating propeller near 30% of the span. A visualization of the propeller–wing system as modeled for this case is provided in Fig. 10 for reference. This result is contrary both in rotation direction and location to the literature on the topic, but is consistent with respect to the trends seen in this study (i.e., is not a single outlier point). With respect to suggestions by Prandtl [10], this result indicates that improvement of the wing efficiency was a more dominant effect in this case. When combined with the structural and control advantages of an inboard propeller, this result is significant. It is also noteworthy when comparing Figs. 7–9 that both the magnitude of the power required and the trends (to a lesser degree) are sensitive to the vertical location of the propeller, in agreement with Kroo [18] as discussed in Sec. II.

To better understand these results with respect to the baseline configuration, a comparison of the wing and propeller performance breakdowns are provided in Tables 4 and 5. Data for both the actual baseline (as validated previously) and for a case with the propeller diameter and spanwise location of the baseline design, but with a QMIL designed propeller, are provided (referred to as *Baseline QMIL*). This second case is provided to isolate the influence of the diameter and location from the propeller planform design.

There are several noteworthy points in Tables 4 and 5. First, in the final operating condition, the lift of all designs varies by less than 1%. Wing drag, on the other hand, varies significantly, with a reduction in both profile and induced drag from the baseline configurations to the optima. The majority of this benefit comes in terms of induced drag. The reduction in drag translates to a reduction in thrust required and thus power required.

To elucidate the reduction in drag, the lift distribution and drag distribution for the QMIL baseline and the two optima are provided in Figs. 11 and 12, respectively. The influence of the propeller slipstream for all three cases is evident in the local increases in lift representing the upward moving swirl component and decreases representing

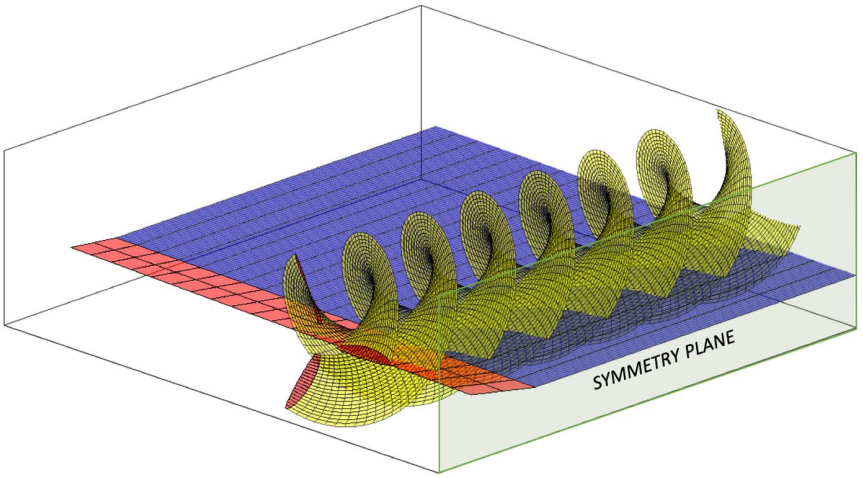

Fig. 10 A visualization of the optimum propeller–wing system identified in this study as modeled with a fixed wake in the HOFW method.

Table 4 Breakdown of wing performance components

Design	Lift, kN	Profile drag, N	Induced drag, N	Nacelle drag, N	Total wing drag, N
Baseline	13.31	134.31	201.29	35.45	371.05
Baseline QMIL	13.31	119.58	192.17	37.07	348.82
Inboard-up optimum	13.31	117.94	146.56	43.04	307.53
Inboard-down optimum	13.31	116.36	137.10	42.59	296.04

Table 5 Breakdown of propeller performance components

Design	Thrust, N	Induced power, kW	Profile power, kW	Total power, kW
Baseline	956.5	79.74	2.72	82.46
Baseline QMIL	926.5	76.07	2.85	78.91
Inboard-up optimum	885.7	74.21	2.96	77.16
Inboard-down optimum	875.2	73.60	2.66	76.27

the downward moving swirl component. The lift distributions are somewhat triangular in nature, with heavier loading in the inboard portion of the wing than would be present in an elliptical distribution, for example. Regardless of the direction of swirl, there is a reduction in drag in the slipstream region for both the inboard-down and the inboard-up minima, as well as in the baseline case.

To further investigate the source of these drag reductions, the breakdown of local drag components is provided in Fig. 13. The profile drag increases in the propeller slipstream for both minima designs, as would be expected due to the increase in dynamic pressure. This increase is more than offset by the reduction in induced drag experienced in this region. Because the result is consistent for both cases, it appears to be driven by the increase in dynamic pressure as well, rather than an influence of swirl. In this case, the authors hypothesize that the benefit is a result of the adjustment of the lift distribution to flatten the relatively steep shedding of vorticity occurring inboard on the wing, where the bound circulation is high. In agreement with Miranda and Brennan [14], it appears that the light loading of the wing tips in this case reduces the effectiveness of the tip-mounted propeller configuration.

In summary, this case illustrated that the potential benefits of the wing-tip-mounted, inboard-up rotating propeller are not general but rather very dependent upon many aspects of the propeller–wing system design. There are interactions between all three variables considered (rotation direction, diameter, and location). In this case, a minimum-induced-loss designed, inboard-mounted, inboard-down rotating propeller improved the aerodynamics of the propeller–wing system by 3.5% over a minimum-induced-loss designed, wing-tip-mounted inboard-up rotating propeller.

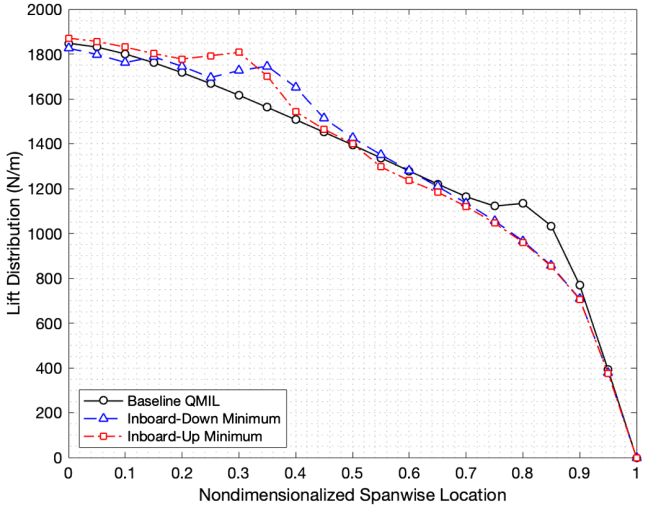

Fig. 11 Time-averaged lift distributions of three notable designs.

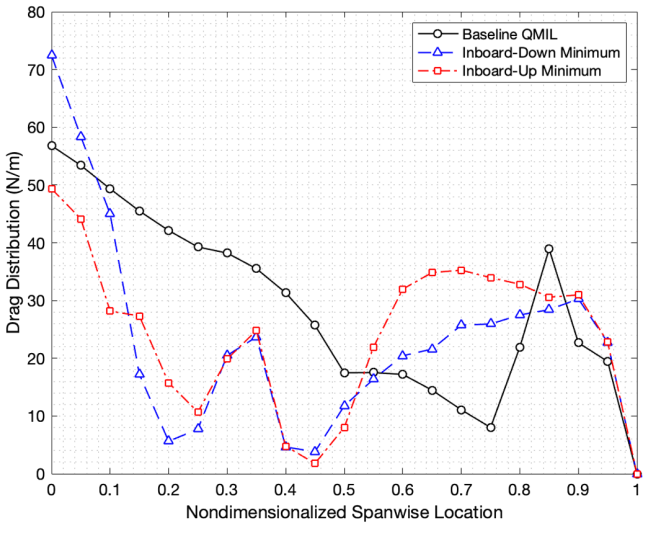

Fig. 12 Time-averaged drag distributions of three notable designs.

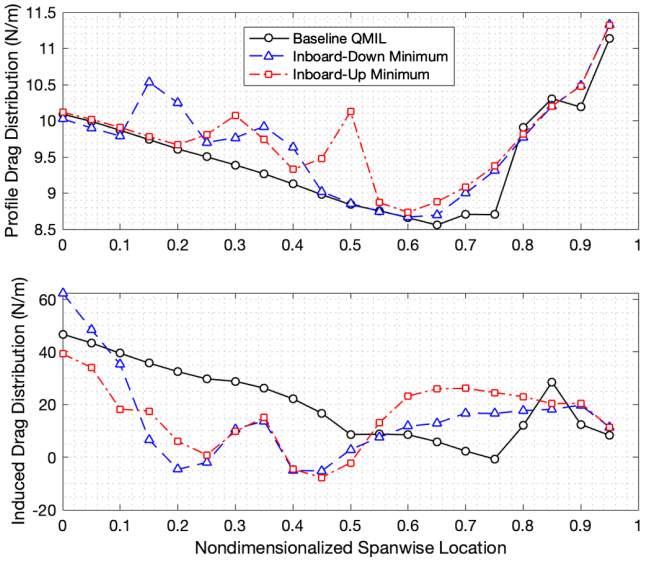

Fig. 13 Breakdown of drag contributions for three notable designs.

V. Conclusions

A new approach to design space exploration for integrated propeller–wing systems has been developed. Development and application of the approach to a test case have resulted in the following conclusions:

1) Because of the complexity of the propeller–wing design space, it is necessary to account for both trim (steady-level flight) and two-sided interactional effects when comparing designs. The authors recommend the use of the trimmed propeller power required as a metric for this purpose. In addition, to ensure that the propeller is not operating significantly off design, the authors recommend including a propeller-design step within the iterative trim process.

2) The prevailing theory that tip-mounted up-inboard rotating propellers are the most efficient configuration was shown to be conditional through the counterexample shown herein and should be applied with caution. In reality, performance trends with respect to propeller diameter, rotation direction, and location depend on the details of both the wing planform and propeller design.

3) In the case of the X-57 cruise configuration and within the bounds of the design space explored, the trimmed propeller power required was shown to be sensitive to the vertical location of the propeller in both magnitude and trends. For this case, the minimum power required configuration was an inboard-down rotating propeller located at approximately 30% of the half-span located 15 cm above the wing. The majority of the benefit was a result of a reduction in induced drag on the wing within the propeller slipstream.

Acknowledgments

The authors gratefully acknowledge support from the following contributors at Bucknell University: Jeremy Dreese (Engineering Computing Support Team), Adit Acharya, Cameron Dennis, and Rich Peterson (undergraduate research assistants) and the department of Mechanical Engineering. The authors also gratefully acknowledge the contributions of Alton Yeung (graduate research assistant, Ryerson University), support through access to the resources of Compute Canada and funding from the Natural Science and Engineering Research Council of Canada (funding reference number RGPIN-2016-03920).

References

[1] Borer, N. K., Patterson, M. D., Viken, J. K., Moore, M. D., Bevirt, J., Stoll, A. M., and Gibson, A. R., "Design and Performance of the NASA SCEPTOR Distributed Electric Propulsion Flight Demonstrator," AIAA Paper 2016-3920, 2016. https://doi.org/10.2514/6.2016-3920

[2] Borer, N. K., Derlaga, J. M., Deere, K. A., Carter, M. B., Viken, S., Patterson, M. D., Litherland, B., and Stoll, A., "Comparison of Aero-Propulsive Performance Predictions for Distributed Propulsion Configurations," AIAA Paper 2017-0209, 2017. https://doi.org/10.2514/6.2017-0209

[3] Deere, K. A., Viken, S., Carter, M., Viken, J. K., Derlaga, J. M., and Stoll, A. M., "Comparison of High-Fidelity Computational Tools for Wing Design of a Distributed Electric Propulsion Aircraft," AIAA Paper 2017-3925, 2017. https://doi.org/10.2514/6.2017-3925

[4] Rothhaar, P., Murphy, P., Bacon, B., Gregory, I., Grauer, J., Busan, R., and Croom, M., "NASA Langley Distributed Propulsion VTOL Tilt-Wing Aircraft Testing, Modeling, Simulation, Control, and Flight Test Development," AIAA Paper 2014-2999, 2014. https://doi.org/10.2514/6.2014-2999

[5] Yeo, H., and Johnson, W., "Performance and Design Investigation of Heavy Lift Tilt-Rotor with Aerodynamic Interference Effects," *Journal of Aircraft*, Vol. 46, No. 4, 2009, pp. 1231–1239. https://doi.org/10.2514/1.40102

[6] Acree, C., "Integration of Rotor Aerodynamic Optimization with the Conceptual Design of a Large Civil Tiltrotor," *Proceedings of the AHS Specialists' Conference on Aeromechanics*, AHS International, Alexandria, VA, 2010.

[7] Wilson, J., "Fly Like a Vulture," *Aerospace America*, Vol. 46, No. 11, 2008, pp. 28–33.

[8] Raymer, D. P., *Aircraft Design: A Conceptual Approach*, 5th ed., AIAA, Reston, VA, 2012, pp. 499–501.

[9] Torenbeek, E., *Synthesis of Subsonic Airplane Design*, Delft Univ. Press, Delft, The Netherlands, 1982, pp. 190–195.

[10] Prandtl, L., "*Mutual Influence of Wings and Propeller*," NACA TN-74, 1921.

[11] Snyder, M. H., and Zumwalt, G. W., "Effects of Wingtip-Mounted Propellers on Wing Lift and Induced Drag," *Journal of Aircraft*, Vol. 6, No. 5, 1969, pp. 392–397. https://doi.org/10.2514/3.44076

[12] Sinnige, T., van Arnhem, N., Stokkermans, T. C. A., Eitelberg, G., and Veldhuis, L. L. M., "Wingtip-Mounted Propellers: Aerodynamic Analysis of Interaction Effects and Comparison with Conventional Layout," *Journal of Aircraft*, Vol. 56, No. 1, 2019, pp. 295–312. https://doi.org/10.2514/1.C034978

[13] Patterson, J. C., and Bartlett, G. R., "Evaluation of Installed Performance of a Wing-Tip-Mounted Pusher Turboprop on a Semispan Wing," NASA TP-2739, Aug. 1987.

[14] Miranda, L., and Brennan, J., "Aerodynamic Effects of Wingtip-Mounted Propellers and Turbines," AIAA Paper 1986-1802, June 1986. https://doi.org/10.2514/6.1986-1802

[15] Veldhuis, L., "Propeller Wing Aerodynamic Interference," Ph.D. Dissertation, Delft Univ. of Technology, Delft, The Netherlands, 2005.

[16] Hooker, J., Wick, A., Walker, J., and Schiltgen, B., "Overview of Low Speed Wind Tunnel Testing Conducted on a Wingtip Mounted Propeller for the Workshop for Integrated Propeller Prediction," AIAA Paper 2020-2673, 2020. https://doi.org/10.2514/6.2020-2673

[17] Cole, J. A., "A Higher-Order Free-Wake Method for Aerodynamic Performance Prediction of Propeller-Wing Systems," Ph.D. Dissertation, Dept. of Aerospace Engineering, Pennsylvania State Univ., University Park, PA, 2016.

[18] Kroo, I., "Propeller-Wing Integration for Minimum Induced Loss," *Journal of Aircraft*, Vol. 23, No. 7, 1986, pp. 561–565. https://doi.org/10.2514/3.45344

[19] Cole, J. A., Maughmer, M. D., Kinzel, M., and Bramesfeld, G., "Higher-Order Free-Wake Method for Propeller-Wing Systems," *Journal of Aircraft*, Vol. 56, No. 1, 2019, pp. 150–165. https://doi.org/10.2514/1.C034720

[20] Drela, M., QPROP Propeller/Windmill Analysis and Design, *Software Package*, Free Software Foundation, Inc., Boston, MA, 2007, http://web.mit.edu/drela/Public/web/qprop/ [retrieved 15 Aug. 2014].

[21] Katz, J., and Plotkin, A., *Low-Speed Aerodynamics*, 2nd ed., Cambridge Univ. Press, Cambridge, U.K., 2001, pp. 230–261.

[22] Bramesfeld, G., "A Higher Order Vortex-Lattice Method with a Force-Free Wake," Ph.D. Dissertation, Dept. of Aerospace Engineering, Pennsylvania State Univ., University Park, PA, 2006.

[23] Bramesfeld, G., and Maughmer, M. D., "Relaxed-Wake Vortex-Lattice Method Using Distributed Vorticity Elements," *Journal of Aircraft*, Vol. 45, No. 2, 2008, pp. 560–568. https://doi.org/10.2514/1.31665

[24] Shevell, R. S., *Fundamentals of Flight*, 2nd ed., Prentice–Hall, Upper Saddle River, NJ, 1989, pp. 181–183.

[25] Bramesfeld, G., and Maughmer, M. D., "Effects of Wake Rollup on Formation-Flight Aerodynamics," *Journal of Aircraft*, Vol. 45, No. 4, 2008, pp. 1167–1173.
https://doi.org/10.2514/1.33821

[26] Kody, F., and Bramesfeld, G., "Small UAV Design Using an Integrated Design Tool," *International Journal of Micro Air Vehicles*, Vols. 4, No. 2, 2012, pp. 151–163.
https://doi.org/10.1260/1756-8293.4.2.151.

[27] Kody, F., Bramesfeld, G., and Schmitz, S., "An Efficient Methodology for Using a Multi-Objective Evolutionary Algorithm for Winglet Design," *Technical Soaring*, Vol. 37, No. 3, 2013, pp. 45–56.

[28] Basom, B., "Inviscid Wind-Turbine Analysis Using Distributed Vorticity Elements," M.S. Dissertation, Dept. of Aerospace Engineering, Pennsylvania State Univ., University Park, PA, 2010.

[29] Maniaci, D., "Wind Turbine Design Using a Free-wake Vortex Method with Winglet Application," Ph.D. Dissertation, Dept. of Aerospace Engineering, Pennsylvania State Univ., University Park, PA, 2013.

[30] Patterson, M. D., "Conceptual Design of High-Lift Propeller Systems for Small Electric Aircraft," Ph.D. Dissertation, Dept. of Aerospace Engineering, Georgia Inst. of Technology, Atlanta, GA, 2016.

[31] Drela, M., XFOIL, *Software Package*, Free Software Foundation, Inc., Boston, MA, 2013, http://web.mit.edu/drela/Public/web/xfoil/ [retrieved 15 Aug. 2014].